Impact Analysis of Polymeric Additive Manufactured Lattice Structures

George Laird[1], Paul DuBois[2]

[1]Predictive Engineering, Inc.
[2]Paul DuBois - Consulting Engineer

1 Abstract

This work was sponsored by the US Army's Natick Soldier Systems Center to investigate additively manufactured lattice structures for improved blunt impact protection for helmets. The idea is simple enough, modern helmets are designed to deflect or mitigate the impact forces due to bullets (high velocity) but not so much for blunt force impacts (lower velocity). In military operations, blunt force impacts are common, albeit sometimes accidently, due to falls or in the rush to enter-exit buildings and vehicles. In combat, flying debris also present challenges to helmet designers where the impacts can be both high- and low-velocity.

Our work was to set the foundation for the exploration of polymeric 3D lattice structures to create the next generation of energy-absorbing helmet liners for military applications. Current foam liners, whether multi-layer or sculptured, all exhibit more-or-less the same energy-absorbing response which is fine for high-energy impacts but lacks the sensitivity for low-energy impacts. If one can move away from the use of foam and toward that of a 3D polymeric lattice structures, then it should be possible to engineer a helmet liner to have a more variable or tailored energy-absorbing response. To create such structures, the additive manufacturing process was used.

The first phase of this test program was to develop a validated FEA model that could be used to predict the impact response of additive manufactured 3D lattice structures. The additive material used for the lattice structure was a methacrylate photopolymer. Standard static compression, tension and bulk modulus testing was performed on 20 mm thick blocks. The same samples were subjected to impact testing at various strain rates. The static and dynamic data was then fitted onto a series of strain-rate dependent curves. The final *MAT_181 law was then validated against these same coupon tests and shown to have good agreement. This material law was then applied to a 3D lattice model for virtual impact testing. Unfortunately the full-on lattice simulations showed no correlation between FEA and test. Although the material law development was accurate to the coupons and the FE model was verified to other numerical tests, it was reasoned that the material characterization had radically changed from large sample (centimeters) to lattice structure (millimeters).

Although this project was a spectacular failure, it did advance our understanding about the challenges of modeling polymeric additive materials. Moving forward, we will be working on a new suite of mechanical tests that would be scale specific to lattice structures… but that will be next year's conference paper.

2 How Could We Go So Wrong?

Not to hold back any surprises, Fig. 1 shows validation results from test coupons and then the additive manufactured samples. The FEA material law was based on the coupons and close agreement was found between FEA and test whereas for the additive manufactured (mfg) structures no agreement was noted. This was quite a surprise to the authors and how we arrived at this discrepancy will be the foundation of this paper.

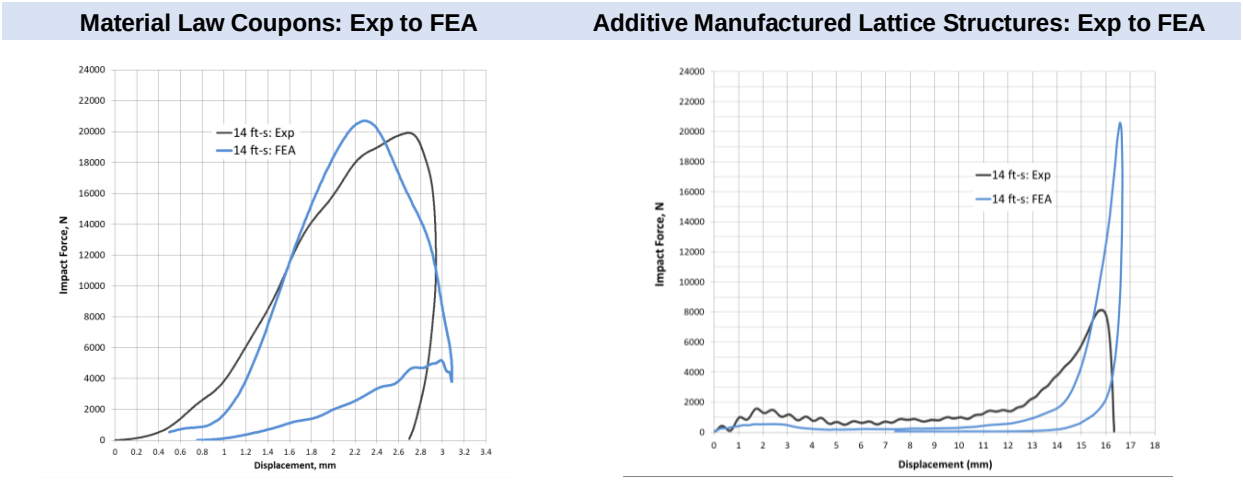

Fig. 1: Validation of FEA model against test coupons and additive mfg structures

3 Why This Work is Important

Additive manufacturing is the break-through technology of the 21st century. Although one can quickly manufacture or print 3D structures of complex shapes, the material characterization and numerical modeling of these structures lags far behind this capability and limits their practical application. The investment and facilities required to characterize these materials lies far outside the realm of industrial research and development and if we are to move additive manufacturing out of the laboratory and into the field, a long-term R&D program is required. Tomorrow's advanced soldier protection systems will not be made from monolithic structures but from combination of materials and shapes that will be impossible to manufacture using 20th century manufacturing techniques; in short, tomorrow is owned by additive manufacturing and currently, we have no good way to create digital prototypes to drive the design process.

What has been learned and will be discussed in this report, is that additive manufactured structures are extremely difficult to experimentally characterize and likewise, extremely difficult to numerically simulate. Fig. 2 provides a summary of our report work from helmet pads to FEA.

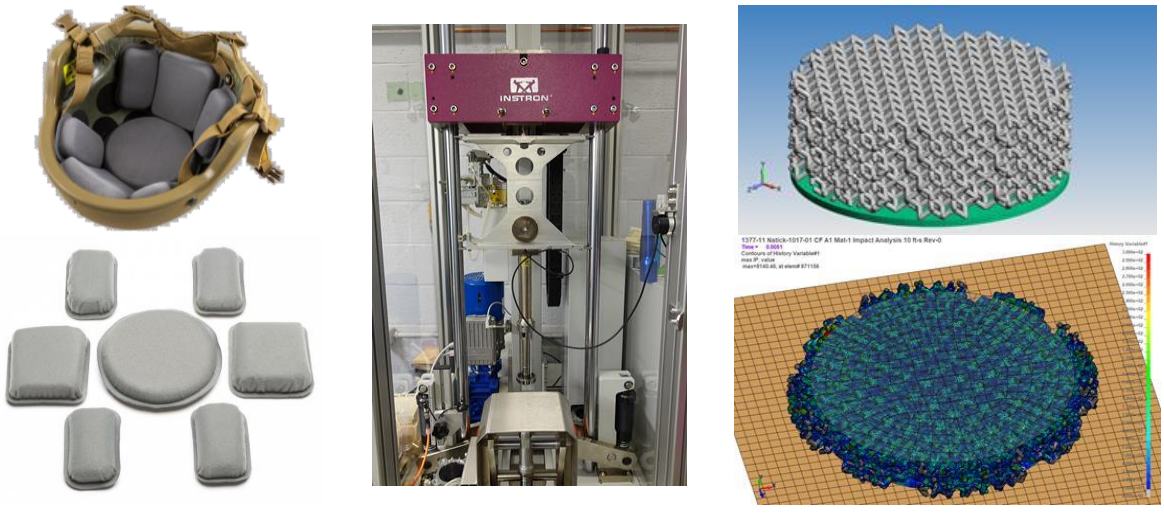

Fig. 2: From combat helmet pads to testing to additive mfg lattice structures to FEA

3.1 Where we are at today

The goal of this work was to use additive mfg structures to create unique stress versus strain responses that would offer improved blunt force impact mitigation. In Fig. 3, a standard foam curve is shown and what is hypothesized as an ideal stress versus strain response curve.

Standard Stress v Strain Response for Foam | **Hypothesized Additive Mfg Response**

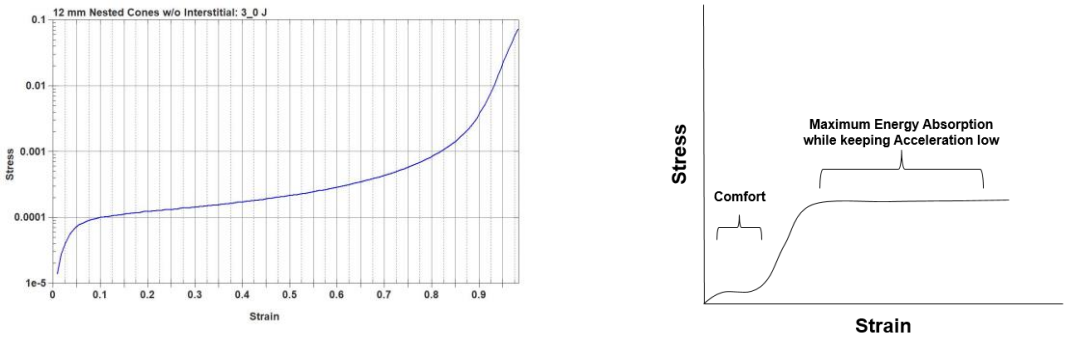

Fig. 3: Standard stress vs strain curve for foam materials and desired curve for blunt force mitigation

In prior work for a sports equipment manufacturer, various foam shapes were investigated to provide improved blunt force energy absorbing characteristics or mitigation. Fig. 4 shows a few of the models that were used in this study. Although extremely good validation was obtained between test and FEA, the stress vs strain response was always, predictably standard with no real improvement in mitigation of the blunt force energy.

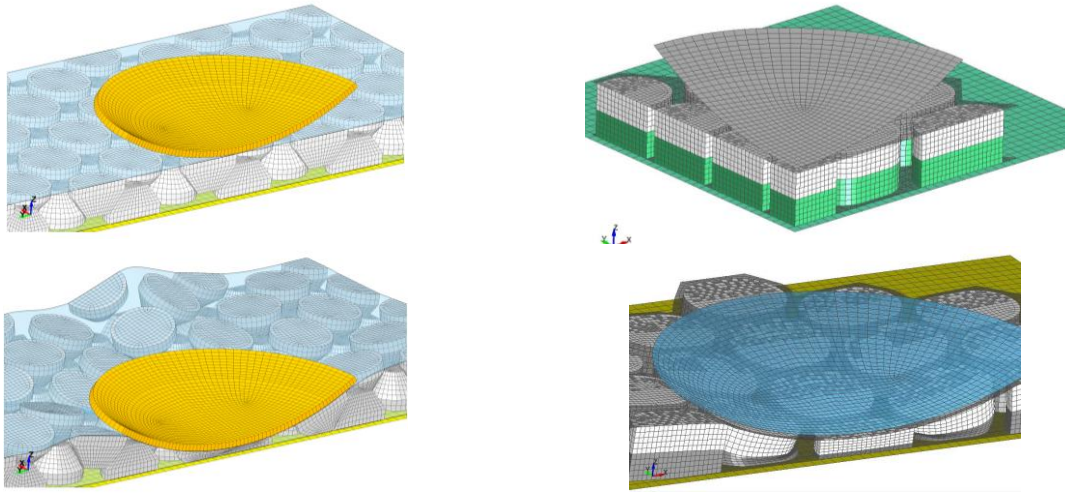

Nestled Cones | **Dual Density Layers**

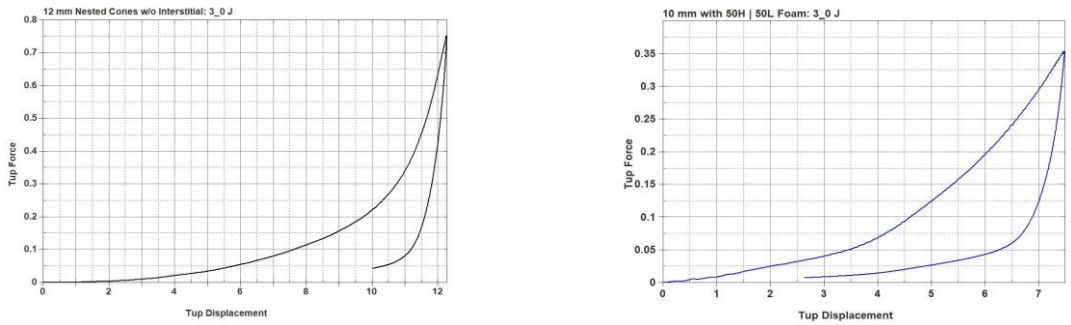

- Fig. 4: Examples of prior work with homogenous foam structures

4 Description of Experimental Test Methods

Experimental tests were performed on standard coupons created by additive manufacturing. The material used in this process was from Formlabs Flexible resin with a trade name of FloFloGro2. Fig. 5 shows the printer and an example 3D lattice structure.

Formlabs Form 2 Printer	Example Additive Mfg 3D Lattice Structure
	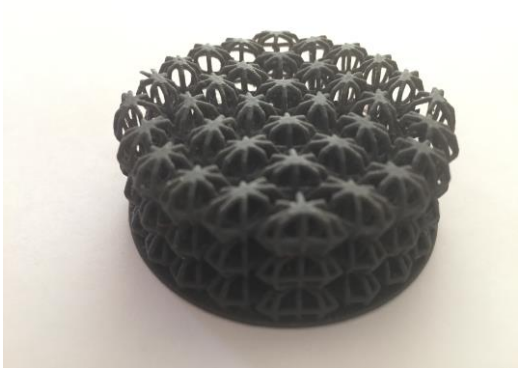

Fig. 5: Formlabs form 2 printer and example 3D lattice structure

4.1 Static Compression Test Data

Static test data using a puck having a 48 mm diameter and 19.15 mm thick is shown in Fig. 6. The raw experimental data was then processed into a clean curve. The last step is to convert the data into engineering stress versus strain data based on the puck's area (1,810 mm^2) and its height (19.15 mm). At maximum load, the stress in the puck is 21.9 MPa at an engineering strain of 52%.

Raw Instron Data	Processed Experimental Data
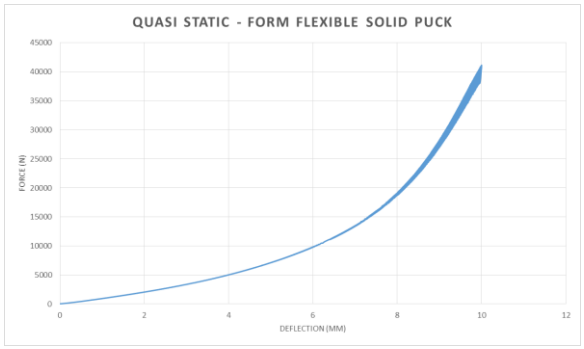	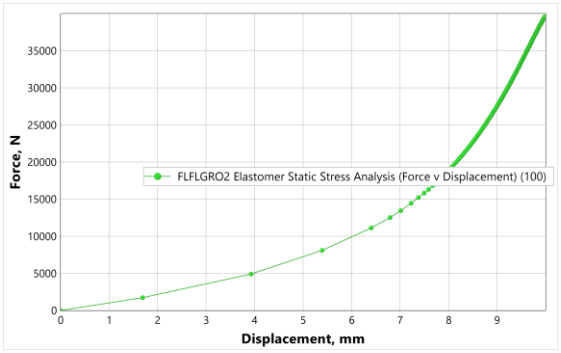

Engineering Stress versus Strain	Static FEA Model
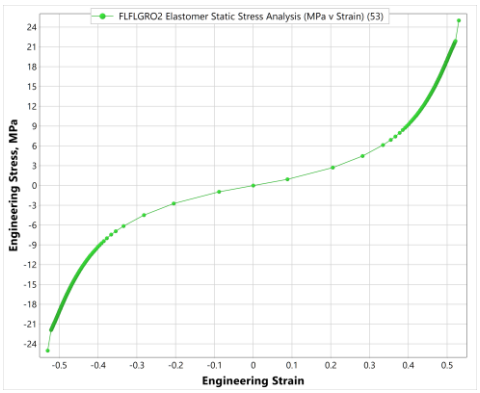	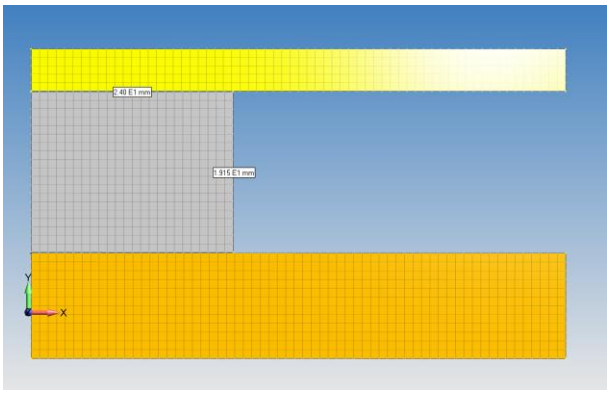

Fig. 6: Static compression test data to FEA

4.2 Experiment to FEA Compression and Tensile Testing

To verify the FEA static material model, the experimental test was simulated. Results from this simulation are shown in Fig. 7. The top image shows the stress in the hockey puck under a 10 mm displacement. It is assumed that the platens do not restrain the elastomeric material. The bottom image shows the experimental and FEA results. The experiment and FEA results align closely. This verifies the FEA material model.
Along the bottom of this figure is the FEA 1/8th symmetric model used for the tensile test. It is based on standard ASTM dimensions.

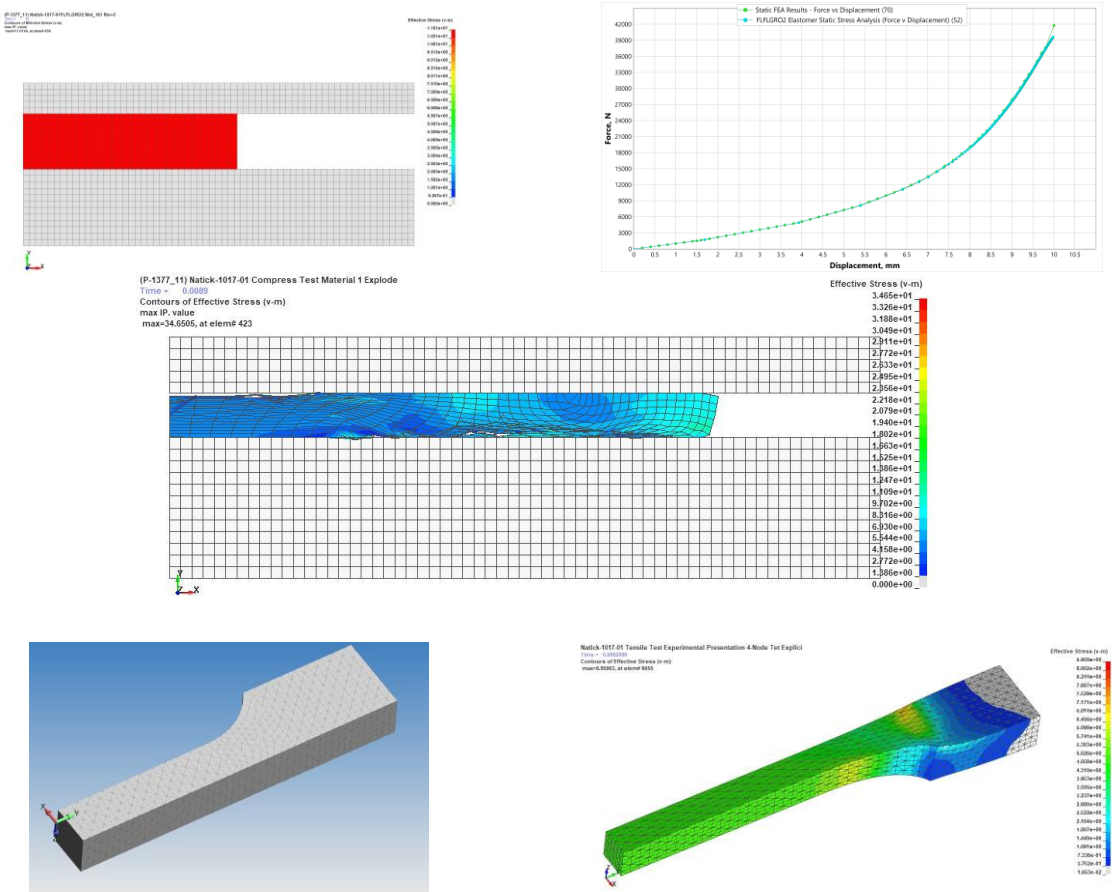

Fig. 7: FEA models for compression and tensile testing with compression experimental data

4.2.1 Validation of Experimental to FEA Results for Coupons

The experimental test data for the tensile and compression tests are shown below in Fig. 8. In both cases the FEA model closely aligns with the experimental test coupon data.

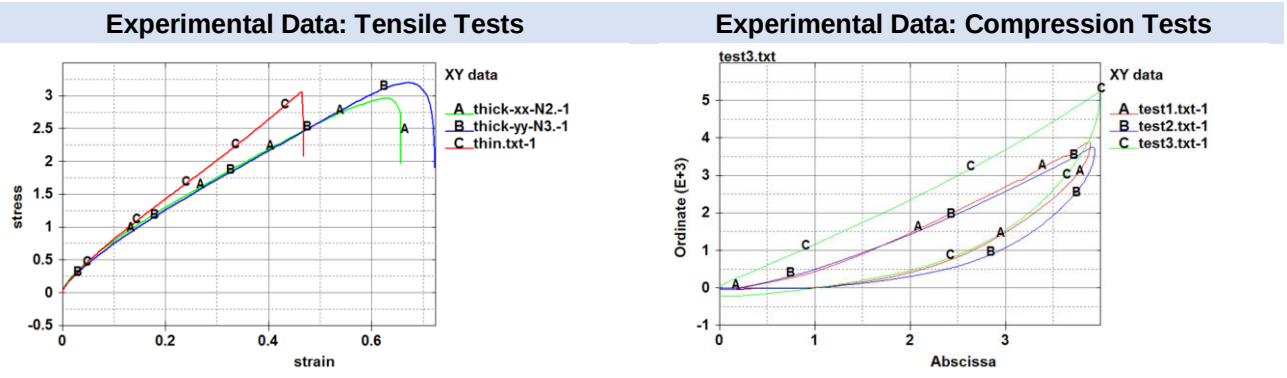

Fig. 8: Tensile and compression experimental test data

4.3 Bulk Modulus Testing

Fig. 9 shows the geometry and mesh setup for the bulk modulus simulation. The maximum plunger load is 40 kN given that the test machine's maximum load capacity is 50 kN. The test plug is 20 mm diameter by 25 mm tall.

Bulk Modulus Fixture Geometry	FEA Model for Bulk Modulus Evaluation	Bulk Modulus Results

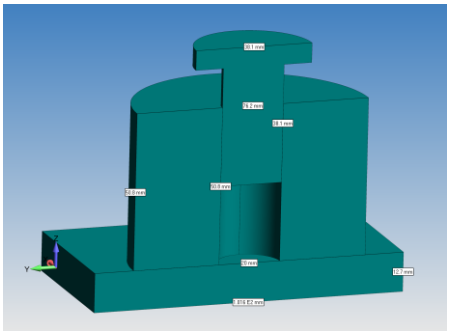

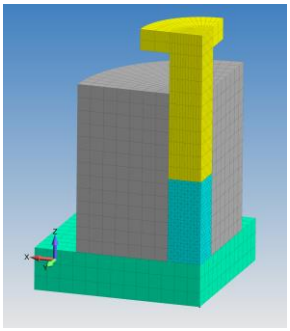

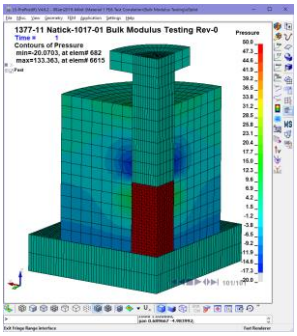

Force versus Displacement Response from Bulk Modulus Evaluation

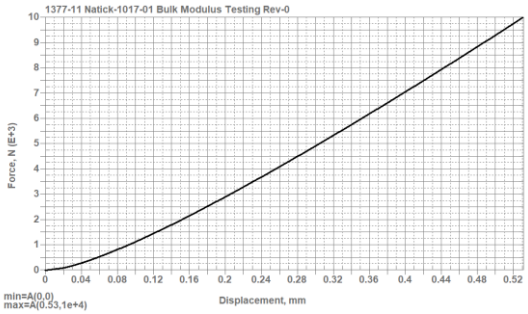

Fig. 9: FEA procedure for development of compression component of material law

4.4 Impact Testing of Elastomeric Materials

Fig. 10 shows the experimental setup used to generate impact data of the various elastomers investigated in this report. Some test specifications: (i) total striker mass = 3.104 kg; (ii) Anvil = 1.00 inch thick stainless steel plate; (iii) Striker diameter = 50mm and (iv) Sample "puck" dimensions = 48 mm OD x 19.05 mm H. The impact rate is by striker head velocity: 10 feet per second (FPS) (3,048 mm/s), 14.1 FPS (4,300 mm/s) and 17.3 FPS (5,270 mm/s).

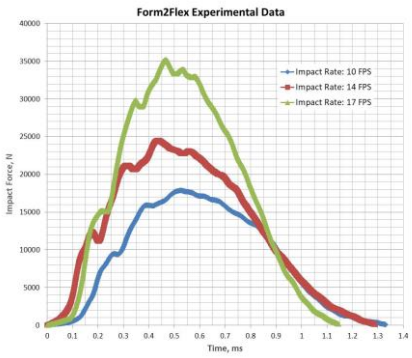

Fig. 10: Experimental test setup for impact testing with test data

4.5 FEA Impact Model

Fig. 11 shows the starting geometry, the idealization process and then the final axisymmetric FEA model. The FEA model shows the puck having a radius of 24 mm and a thickness of 19 mm. The *MAT_181 material curves developed from the experimental tests on coupons were then applied to this FEA model.

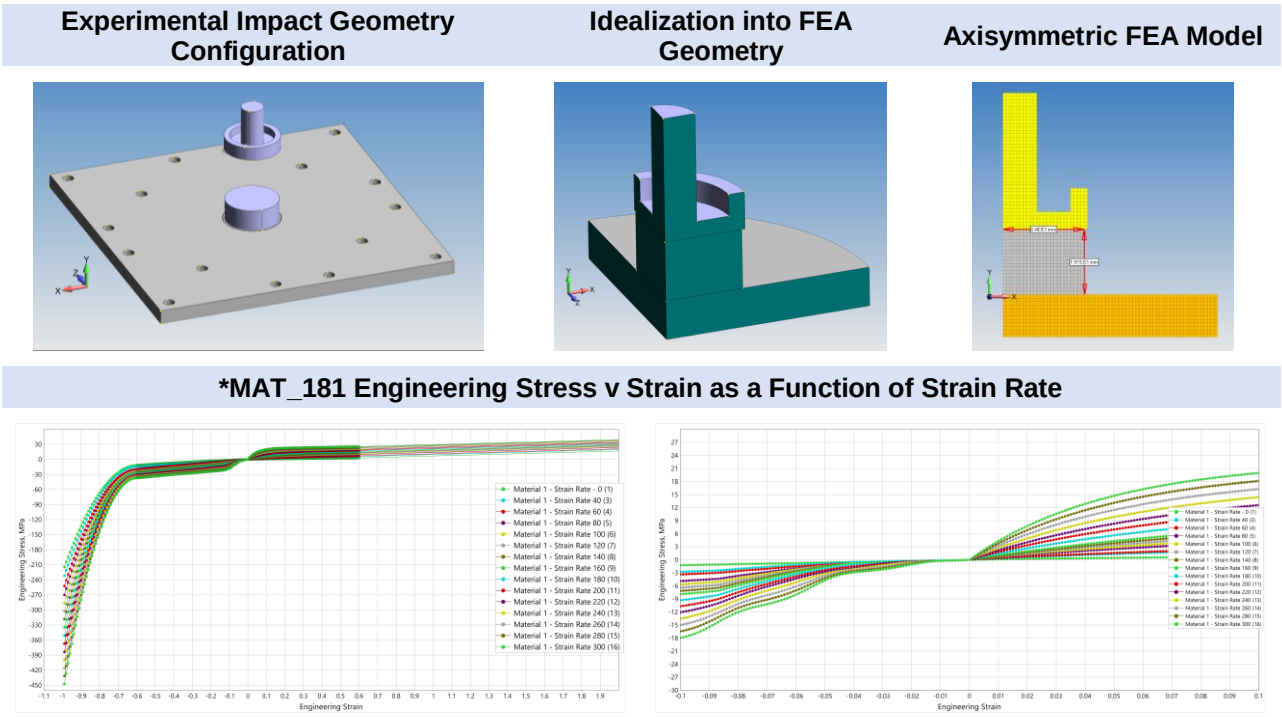

*Fig. 11: FEA impact model and engineering stress v strain curves for *MAT_181 material law*

5 Experiment to FEA Correlation

Fig. 12 provides a graphical summary of the material modeling work in two graphs. The graphs show the material model correlation to impact tests at 10, 14 and 17 ft/s.

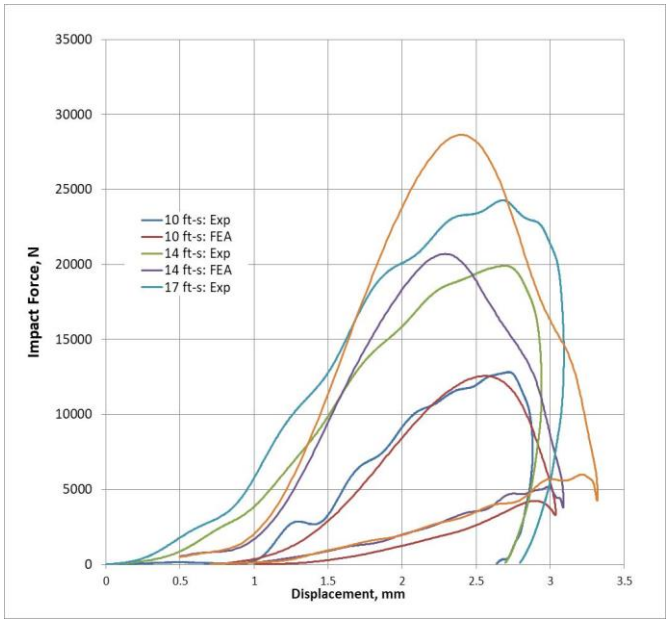

Fig. 12: Overlay of FEA and Experimental curves at three different velocities

6 Impact Analysis of Additive Manufactured 3D Lattice Structures

Fig. 13 shows the additive manufactured (mfg) 3D lattice structures that were impacted in this study. The lattice structure was meshed with 4-node tetrahedrals (ELFORM=13). A mesh convergence study was performed to arrive at a converged mesh density for each lattice structure. The scale of the lattice members range from 1 (CF A1) to 2 mm (CVC E1). Symmetry could not be exploited given the non-symmetric nature of the lattice structures.
The 3D lattice structures were manufactured with a base attached to the bottom layer (first row of image). The flat base shown in the second row of images is the idealized impact platen (rigid material – *MAT_20) having a mass of 3.104 kg.

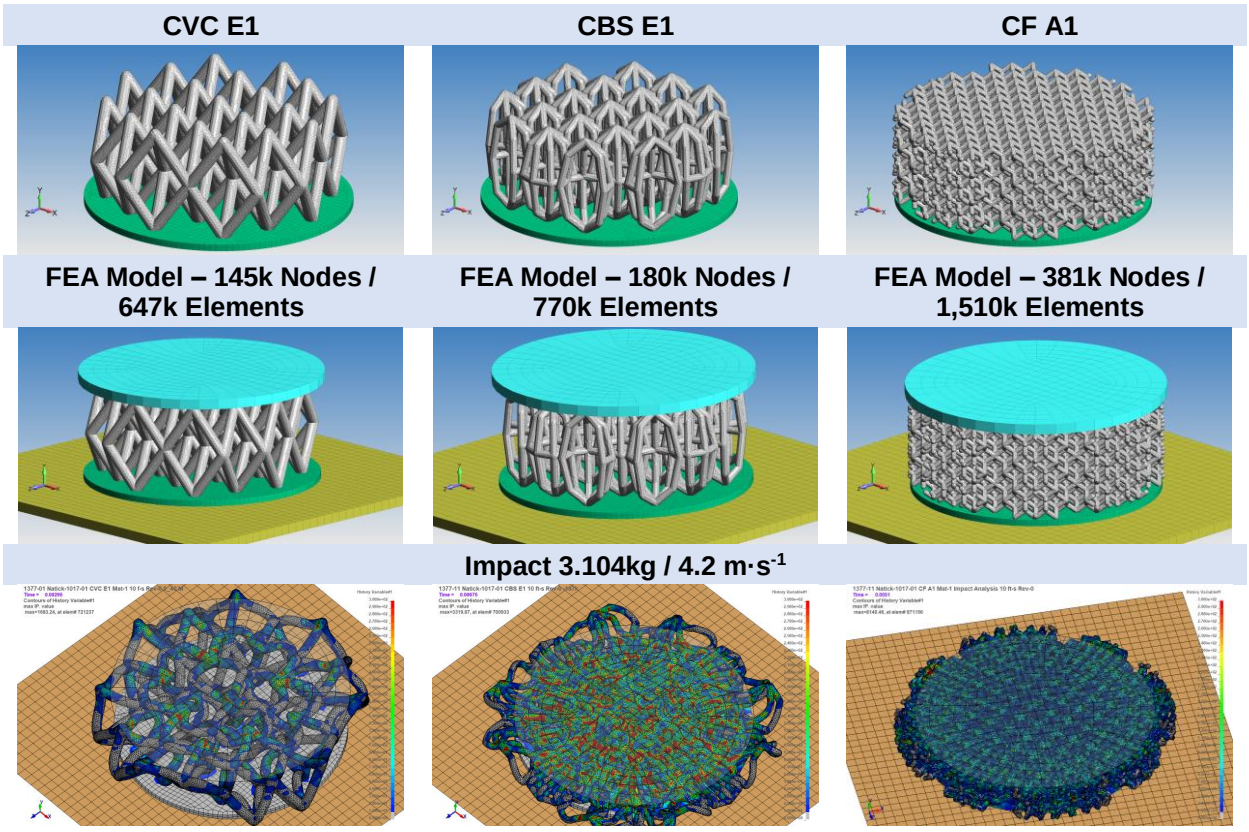

Fig. 13: Additive mfg 3D lattice structures as impacted at 4.2 m/s

6.1 LS-DYNA Analysis Notes

Given the use of ELFORM=13 for the thin lattice structures, our initial concern was meshing but during this investigation we determined that contact between individual mesh facets was also a controlling factor in limiting negative sliding interface energy. These issues were addressed by the classical method of mesh, re-mesh and then re-mesh some more, as shown in Fig. 14. Conventual mass scaling was also employed and was checked by contouring the added mass density and limited to 5% of the additive mfg part and not the system mass.

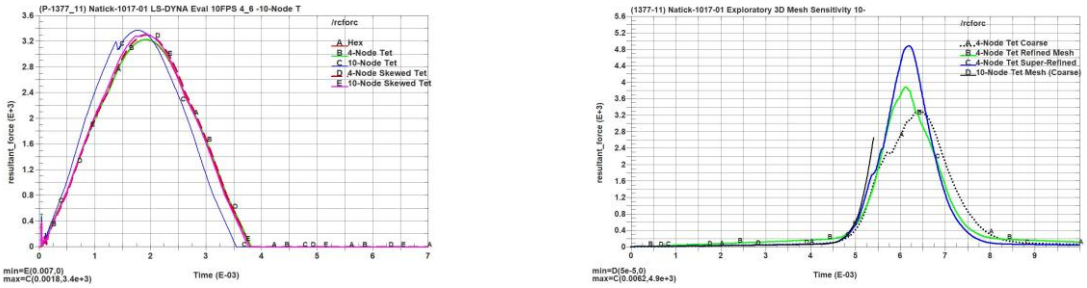

Fig. 14: Element quality, formulation and mesh density investigation

6.1.1 Meshing

Fig. 15 shows an example of the meshing procedure presented using the CBS E1 geometry. The lattice structure was first seeded with a global mesh size of 0.45 mm. After which, 4-noded solid tetrahedral elements were meshed onto the surface of the solid geometry. The element quality was checked by contouring the mesh with the Jacobian.

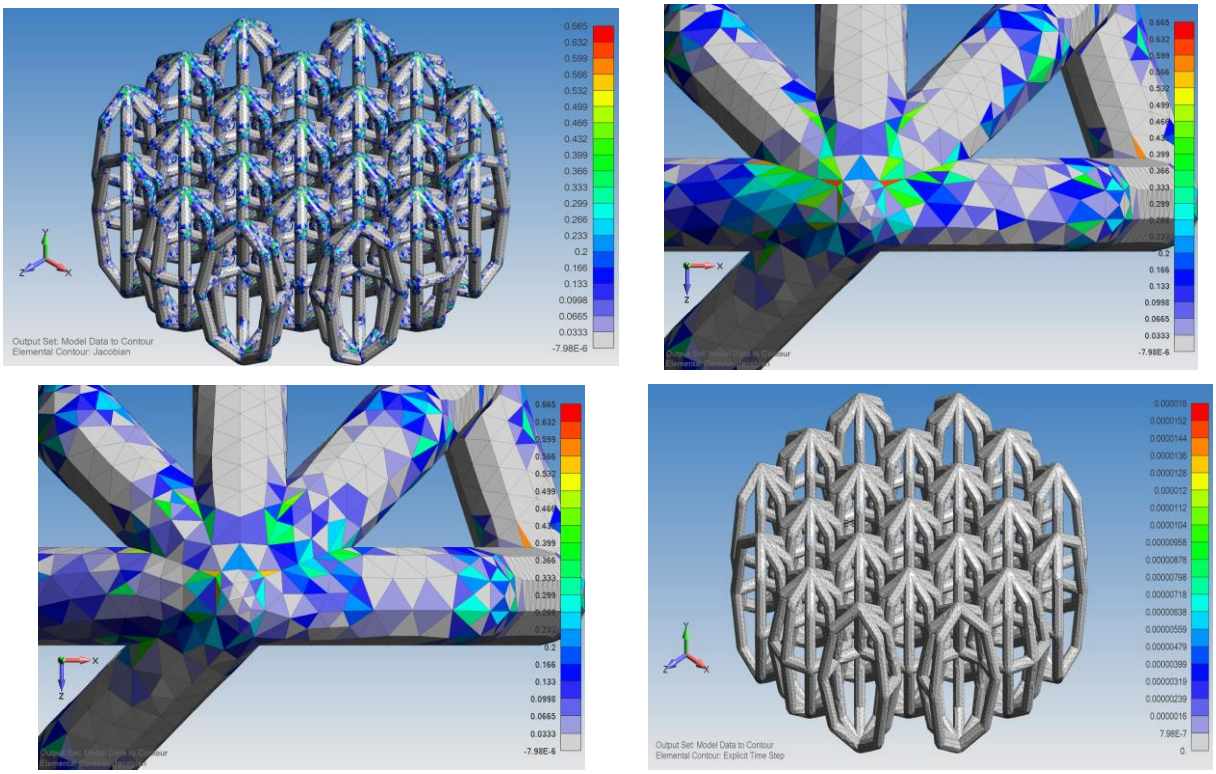

Fig. 15: Element quality checks using Jacobian and explicit time step contours

Table 1 provides an idea on how the mesh was converged based on mesh sizing and timestep. The objectives were to lower negative sliding interface energy and contact force.

Table 1: An example of the mesh convergence and analysis objectives

Trial	No. Nodes	Contact Type	_TIMESTEP	SLE/IE (k)	Max Force (kN)
1	87k	SOFT=2	5e-8	0.84/13.4	10.6
2	109k	SOFT=2	5e-8	0.82/13.4	10.0
3	146k	SOFT=2	5e-8	0.85/13.0	10.4
4	146k	SOFT=2	2.5e-8	0.72/13.0	10.0
5[1]	145k	SOFT=2	5e-8	0.54/14	8.3
6	145k	SOFT=2	1.5e-7	0.29/11	8.5

[1]Friction value increased from 0.3 (used in all models) to 1.0 as an upper bound of reality.

7 FEA Impact Results

7.1 3D Additive Mfg Lattice Structure - CVC E1

Impact test results for CVC E1 are shown in Fig. 16 through the time sequence up to full impact. The first image is the force versus displacement curve for the impact followed by images of the lattice structure being compressed. The mesh is contoured with the strain rate. The legend is capped at 300 strain/sec and is the maximum strain rate that was captured in the material law formulation. The ratio of SLE/IE = 0.8k/13.0k and the maximum impact force is 10 kN.

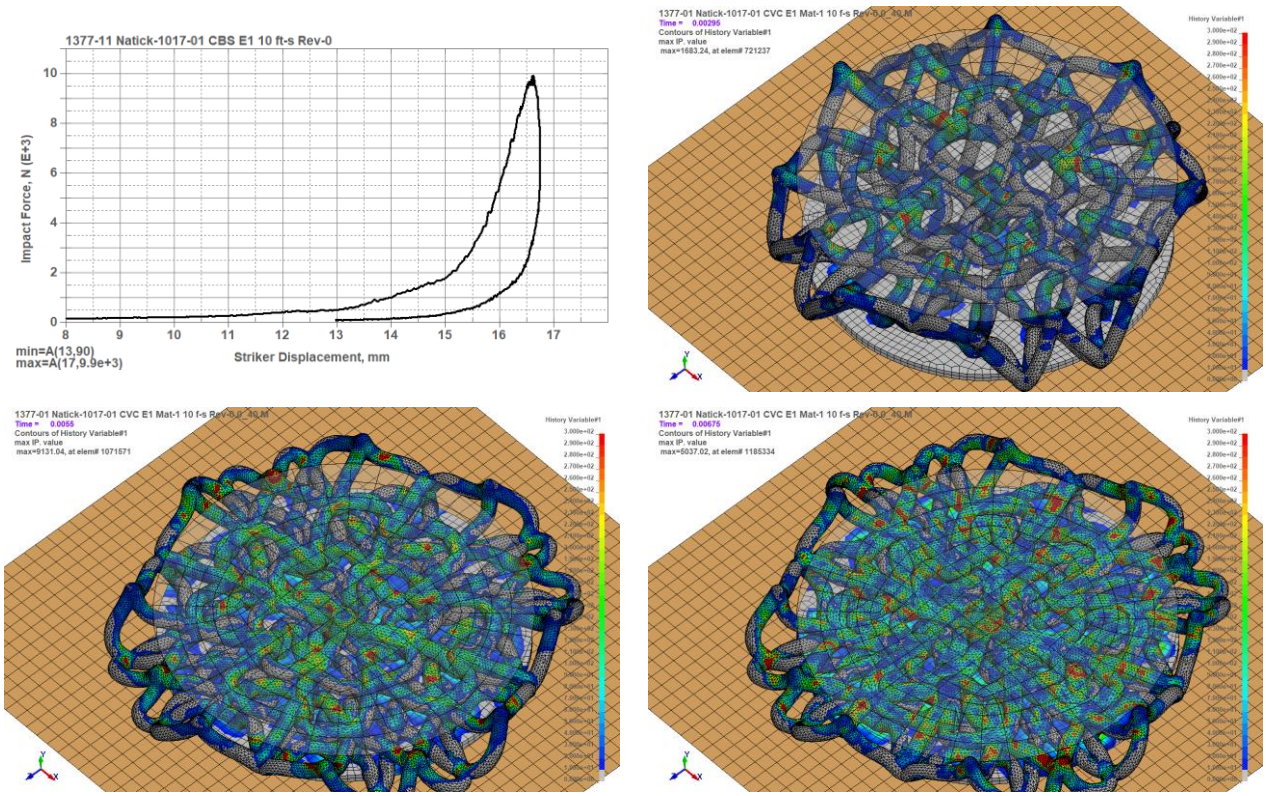

Fig. 16: Impact analysis of CVC E1 at 4.2 m/s

7.2 3D Additive Mfg Lattice Structure - CBS E1

Impact test results for CBS E1 are shown in Fig. 17 through the time sequence up to full impact. The first image is the force versus displacement curve for the impact followed by images of the lattice structure being compressed. The mesh is contoured with the strain rate. The legend is capped at 300 strain/sec and is the maximum strain rate that was captured in the material law formulation. The ratio of SLE/IE = 1.5k/13k and the maximum impact force is 13 kN.

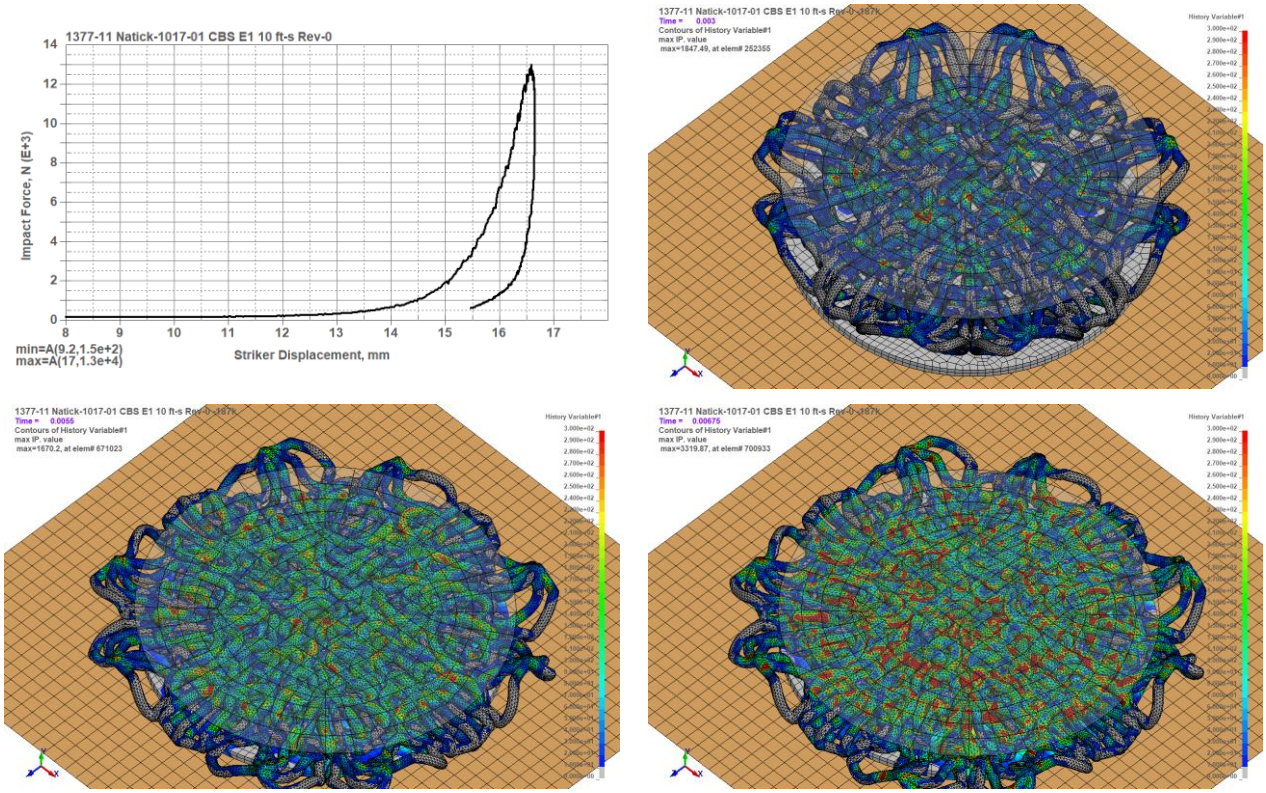

Fig. 17: Impact analysis of CBS E1 at 4.2 m/s

7.3 3D Additive Mfg Lattice Structure - CF A1

Impact test results for CF A1 are shown in Fig. 18 through the time sequence up to full impact. The first image is the force versus displacement curve for the impact followed by images of the lattice structure being compressed. The mesh is contoured with the strain rate. The legend is capped at 300 strain/sec and is the maximum strain rate that was captured in the material law formulation. The ratio of SLE (Mat 1 only)/IE = 0.8k/13k and the maximum impact force is 8.4kN.

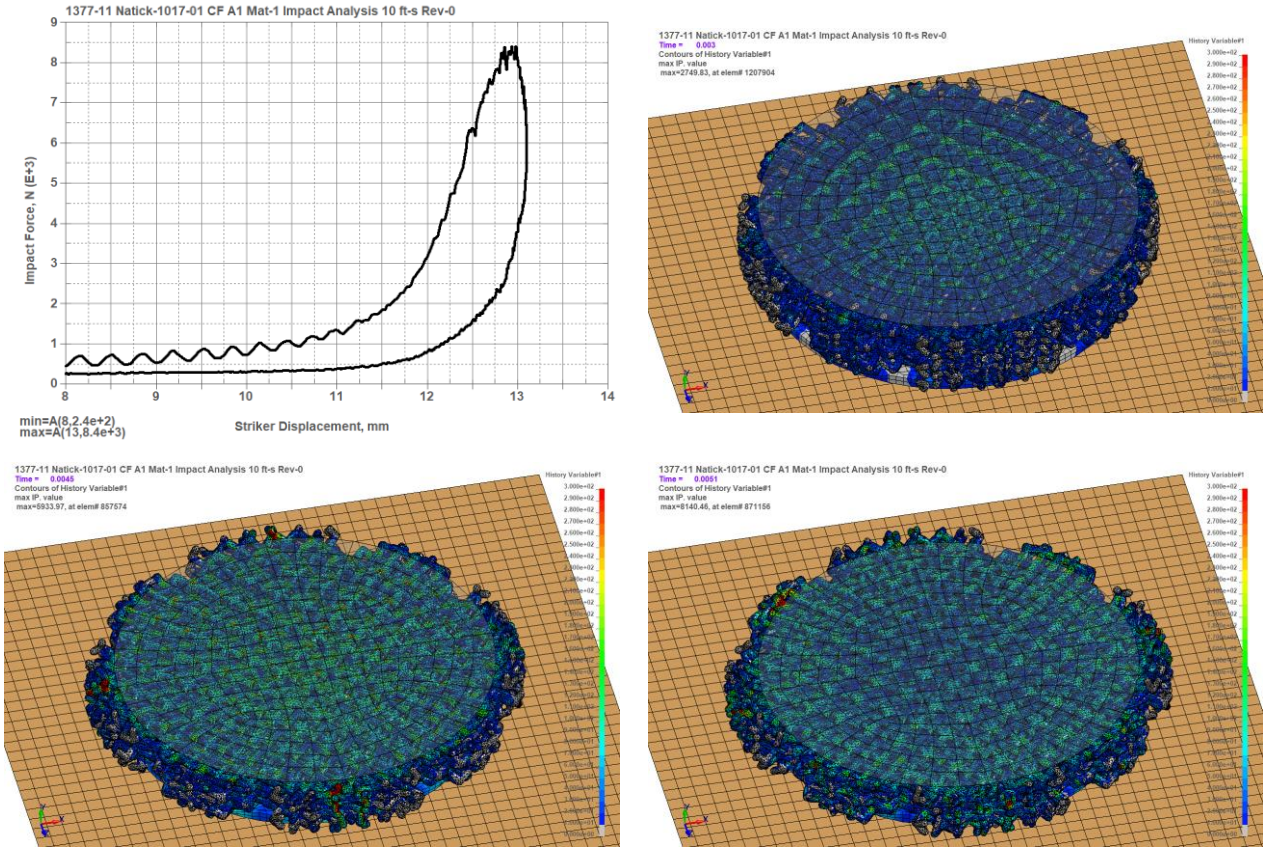

Fig. 18: Impact analysis of CF A1 at 4.2 m/s

8 Summary

Table 2 presents a summary of the results as tabulated per impact velocity versus maximum impact force. As seen, the simulation over predicted the maximum impact force by significant margin.

Table 2: Summary of Results

Velocity	CVC E1		CBS E1		CF A1	
	Exp, kN	FEA, kN	Exp, kN	FEA, kN	Exp, kN	FEA, kN
10 ft/s (3 m/s)	2.1	10	4.6	13	5.5	8.4
14 ft/s (4.3 m/s)	8.1	25				
17 ft/s (5.2 m/s)	14.3	45				

8.1 Why Correlation Between Test and FEA Was Not Possible

Fig. 19 sums up the comparison between the CVC E1 FEA and test by showing the impact force versus time. The difference is too large to explain by modeling assumptions. For example, by varying the friction value from 0.3 to 1.0, we could drop the maximum force from 10 to 8.3 kN, however, this is a long way from the experimental value of 2.1 kN. There is just something fundamentally different between the FEA model and the test.

Material Law Coupons: Exp to FEA | **Additive Manufactured Lattice Structures: Exp to FEA**

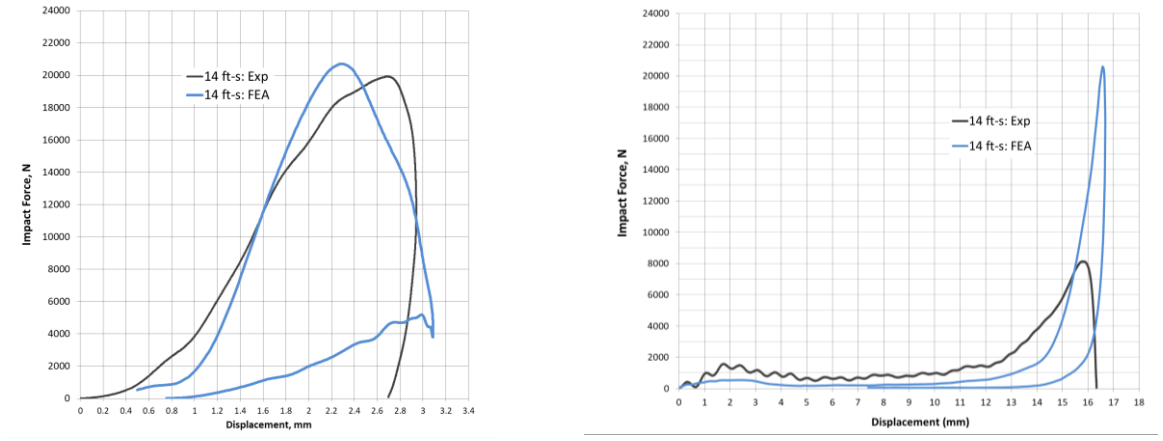

Fig. 19: Comparison of FEA to test results using the CVC E1 geometry

In summary of our investigation why the FEA model fails to correlate with the test results, Fig. 20 provides a graphical summary of the challenges that were faced with model to test correlation. In brief, two dominant challenges were noted: (i) test data was taken on large, monolithic blocks (19 mm thick x 50 mm diameter) while the test articles were lattices having member diameters of 1 mm and (ii) material property data was gathered at a limited strain range from -0.6 to +0.6 whereas the analysis work showed that the lattice structures would exhibit much higher strain ranges from -0.9 (or higher) to likewise +0.9 (or higher).

Material Data from 50 mm Diameter Blocks | **Impact Test Articles are Lattices of 1 mm**

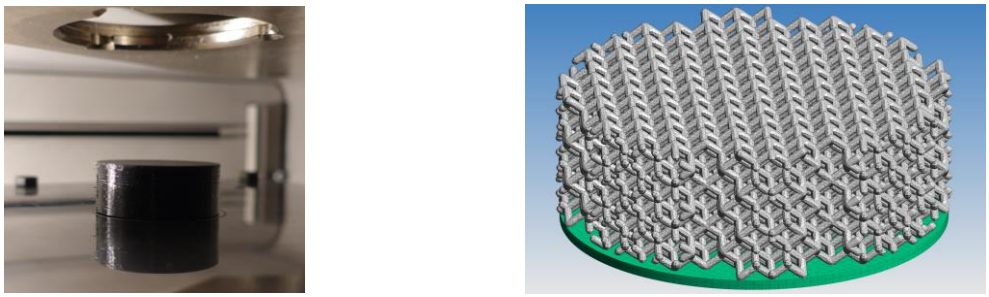

Test Data is between -0.6 and +0.6 Strain | **At 10 ft/s, the FEA Strain Far Exceeds Test Data**

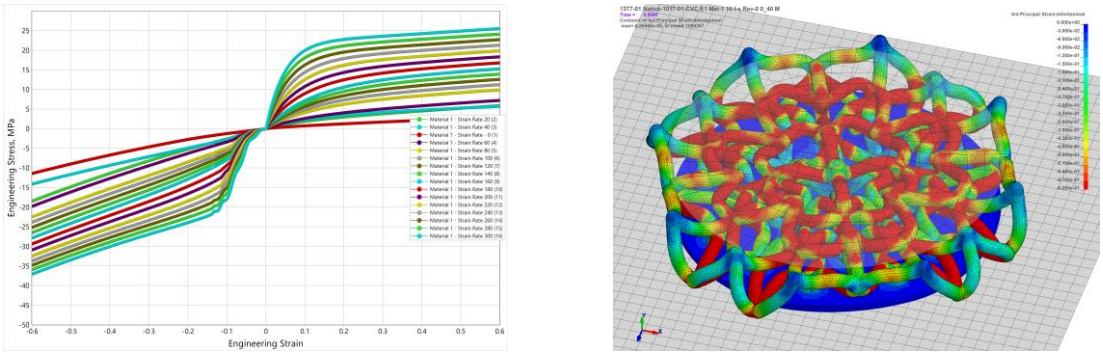

Fig. 20: Graphical summary of why correlation was not possible

8.2 Recommendations for Follow-On Work

Rate dependent material properties for Material 1 were found through impact testing of a puck. The measured data from this test is not representative of the lattice structure as the block's size was shown to be too large (48mm OD x 19.05mm H) for comparison with the strut diameter (1.48 mm) of the lattice. Materials manufactured by additive processes are inherently subjected to localized flaws due to the nature of how each subsequent layer is built on top of one another. Thus, material properties may be inconsistent between each production. However, if the structure is sufficiently large, the overall macromechanical behavior may be unaffected by these flaws. If one is trying to capture the behavior of the lattice, non-standard tests should be performed to build the non-standard material laws.

9 Acknowledgments

The authors would like to thank the US Army, Natick Soldier Systems Center for the engineering and financial support of this work in improving the blunt force impact performance of combat helmets.